

ESI-619
OUT-4102-77
MZ-TH/98-42
hep-th/9810087
13 October 1998

Renormalization automated by Hopf algebra

D. J. Broadhurst¹⁾ and D. Kreimer²⁾

Erwin Schrödinger Institute, A-1090 Wien, Austria

Abstract It was recently shown that the renormalization of quantum field theory is organized by the Hopf algebra of decorated rooted trees, whose coproduct identifies the divergences requiring subtraction and whose antipode achieves this. We automate this process in a few lines of recursive symbolic code, which deliver a finite renormalized expression for any Feynman diagram. We thus verify a representation of the operator product expansion, which generalizes Chen's lemma for iterated integrals. The subset of diagrams whose forest structure entails a unique primitive subdivergence provides a representation of the Hopf algebra \mathcal{H}_R of undecorated rooted trees. Our undecorated Hopf algebra program is designed to process the 24,213,878 BPHZ contributions to the renormalization of 7,813 diagrams, with up to 12 loops. We consider 10 models, each in 9 renormalization schemes. The two simplest models reveal a notable feature of the subalgebra of Connes and Moscovici, corresponding to the commutative part of the Hopf algebra \mathcal{H}_T of the diffeomorphism group: it assigns to Feynman diagrams those weights which remove zeta values from the counterterms of the minimal subtraction scheme. We devise a fast algorithm for these weights, whose squares are summed with a permutation factor, to give rational counterterms.

¹⁾ D.Broadhurst@open.ac.uk; <http://physics.open.ac.uk/~dbroadhu>
permanent address: Physics Dept, Open University, Milton Keynes MK7 6AA, UK

²⁾ Dirk.Kreimer@uni-mainz.de; <http://dipmza.physik.uni-mainz.de/~kreimer>
Heisenberg Fellow, Physics Dept, Univ. Mainz, 55099 Mainz, Germany

1 Introduction

Perturbative quantum field theory (pQFT) entails the process of renormalization: the iterated subtraction of subdivergences of Feynman diagrams, culminating in the subtraction of an overall divergence (or addition of a counterterm) that renders each diagram finite and delivers its contribution to the appropriate renormalized Green function. Many people helped to develop this process, though it has become customary to record the work of Bogoliubov and Parasiuk [1], Hepp [2], and Zimmermann [3] (BPHZ), completed by the forest formula in [3], almost 30 years ago. A review is provided by the textbook of Collins [4]. In addition to the BPHZ formalism one needs analysis, to evaluate regularized expressions for the bare diagrams, prior to renormalization. Much progress has been made in this direction by combining dimensional regularization [5] and integration by parts, for massless [6] and massive [7, 8, 9] diagrams with up to 3 loops, together with more *ad hoc* techniques at higher loops. Since 1981 it was possible, in principle, to obtain the 4-loop β -function of QCD by combining the BPHZ formalism with the algorithm of [6] for massless 3-loop 2-point functions in $D := 4 - 2\epsilon$ spacetime dimensions. Yet not until very recently was a result obtained in [10], and even there the BPHZ formalism was not fully exploited. This serves as an indication of the challenge of *organizing* renormalization.

In this paper, we exploit the work in [11, 12, 13, 14], which shows that the joblist of renormalization is encapsulated by the coproduct, Δ , of the Hopf algebra of decorated rooted trees and that counterterms are given by its antipode, S . We show how truly simple it is to automate renormalization by recursive definitions of Δ and S and hence to calculate the contribution of any diagram to a renormalized Green function, in any situation where analytic methods are adequate to evaluate the regularized bare diagrams entailed by Δ . We emphasize that in this work we use only well-tried analytic methods. Our aims are to make transparent the Hopf algebra of renormalization, to program it efficiently, to apply the program to cases where analysis is possible at large numbers of loops, and to report the first fruit of the process of discovery that is thereby enabled.

In sect. 2 we review 4 crucial formulæ from [11, 12], which capture the entirety of renormalization, and rewrite them as a few lines of code in the symbolic manipulation language REDUCE [15], whose translation to other languages should present little difficulty to readers with other preferences. In sect. 3 we give a representation of the operator product expansion, recently found by DK [14] in the course of extending Chen's lemma [16] on iterated integrals, and hence providing a powerful test of the correctness of our code. In sect. 4 we specialize to the Hopf algebra of undecorated rooted trees, where analytic methods and efficient programming allow us to study its 7,813 Feynman diagrams with loop numbers $n \leq 12$ in a wide variety of field theories and renormalization schemes. In sect. 5 we report our first discovery with this new tool, by showing the remarkable simplification that results when one combines diagrams with the weights specified by Connes and Moscovici [17], in their study of the subalgebra entailed by the diffeomorphism group. Sect. 6 offers conclusions and suggestions for further study.

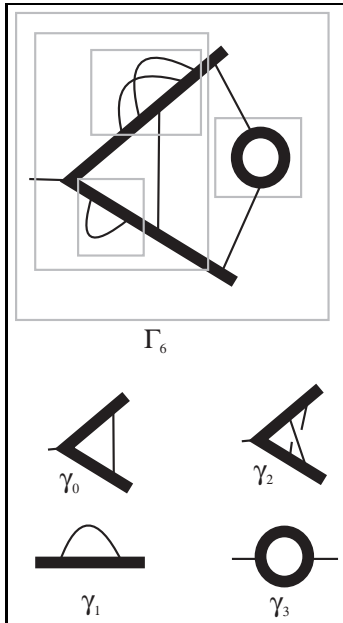


Figure 1: The divergences in Γ_6 are generated by 4 skeleton diagrams.

2 Renormalization by Hopf algebra

The divergence structure of a Feynman diagram is naturally represented by a tree [12], whose vertices (or nodes) represent primitive divergences, with edges connecting vertices in a manner that encodes the nesting (or forest structure) of subdivergences. Each primitive divergence is associated with a skeleton diagram [18], free of subdivergences. To distinguish these we need labels, γ_k . Fig. 1 gives an example from QED, entailing one-loop skeleton diagrams, γ_1 and γ_3 , in the electron and photon propagators, and one- and two-loop skeleton diagrams, γ_0 and γ_2 , in the coupling. The assignment of labels is arbitrary, so long as it permits no confusion. Now consider the 6-loop diagram of Fig. 1. How shall we encode its divergence structure?

One obvious method is to form a list¹:

$$\Gamma_6 = \{0, \{3\}, \{0, \{1\}, \{2\}\}\} \quad (1)$$

The first element of the list is a label, which tells us in this case that the subdivergences reside inside the one-loop skeleton for the coupling. The rest of the list consists of sublists. The first of these is $\{3\}$, which encodes the one-loop primitive divergence in the photon propagator; the second is $\{0, \{1\}, \{2\}\}$, which we parse in exactly the same manner as before: it tells us that inside a one-loop coupling skeleton there reside a one-loop electron-propagator skeleton and a two-loop coupling skeleton. It is also rather convenient that this iterated structure, list=head+sublists, allows us to preserve the order of sublists, which may later be useful in taking traces over spins.

¹In [11] the equivalent information was encoded by parentheses, written in the reverse order. For present purposes, it is more efficient to work with lists, with the outermost label at the head.

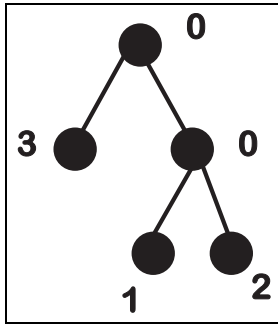


Figure 2: Divergences encoded by a rooted tree, corresponding to the list (1).

An equally obvious, and entirely equivalent, coding is provided by the rooted tree of Fig. 2. It grows (downwards!) from the root 0, which has a pair of branches. Each of these branches is itself a rooted tree: the first has root 3, but no branches; the second has root 0 and branches which are the branchless trees with roots 1 and 2. Clearly, there is a trivial translation between the structure $\text{tree}=\text{root}+\text{branches}$ and the structure $\text{list}=\text{head}+\text{sublists}$ in (1). In each case there is a feature which encapsulates the forest structure of divergences: each branch is itself a tree; each sublist is itself a list.

We shall present the structure of the Hopf algebra in terms of trees, roots, and branches (which are trees); we shall encode it in terms of lists, heads, and sublists (which are lists). In [12, 13] it is shown that overlapping divergences are accommodated by this iterative structure, since they require, at most, a sum of lists of decorations.

2.1 Coproduct

Let $a \in \mathcal{A}$ be a tree, where \mathcal{A} is the algebra of trees, with a product that corresponds merely to the commutative product of the associated Feynman diagrams. A coproduct $\Delta(a) \in \mathcal{A} \otimes \mathcal{A}$, which is not cocommutative, is defined recursively by [11, 12]

$$\Delta(a) = a \otimes e + id \otimes B_r^+(\Delta(B^-(a))) \quad (2)$$

where e is the empty tree (evaluating to unity); id is the identity map in \mathcal{A} ; r is the root of a ; $B^-(a) \in \mathcal{A}$ is the product of the branches of a ; and B_r^+ is the operator that maps any element $c \in \mathcal{A}$ to the tree with root r and branches c . The recursion terminates with

$$\Delta(e) = e \otimes e \quad (3)$$

and is effected by applying the product rule

$$\Delta(b) = \prod_k \Delta(b_k) \quad (4)$$

to the product of branches $b = \prod_k b_k$ obtained by removing the root r of a , and then recombining the products on the right of the tensor product with the original root r .

It was shown in [11] that $\Delta(a)$ generates the joblist of the practical field theorist engaged upon the renormalization of a Feynman diagram with divergence structure given

by the tree a . On the left of the tensor product reside (products of) subdiagrams requiring counterterms; on the right reside diagrams in which these subdiagrams shrink to points. Most of us will testify, if pressed, that it is perilously easy to forget where one has reached when subtracting subdivergences by hand. On the other hand, a correctly programmed recursive procedure, in a suitable symbolic manipulation language, will not lose track. An implementation in REDUCE is provided by

```

for all a,b such that first a=af let A2 a*A2 b=A2 append(a,{b});
procedure D a;
A1 a+sub(af=first a,A2{af}*for k:=2:length a product D part(a,k));

```

where $A1$ and $A2$ are operators that hold lists on the left and right of $\mathcal{A} \otimes \mathcal{A}$ and af is a dummy argument that is replaced by `first a` after each recursion. The `let` statement in the first line sweeps up products on the right of $\mathcal{A} \otimes \mathcal{A}$. In the body of the procedure, the list representing the tree is beheaded by starting at `k:=2`; the product of coproducts of sublists is taken; then product terms on the right are reheaded by the original root. This generates the joblist of renormalization, which finally reads, in Sweedler notation [12]

$$\Delta(a) = \sum_k a_k^{(1)} \otimes a_k^{(2)} \quad (5)$$

with products of trees on the left, and single trees on the right, of the tensor product.

2.2 Antipode

An antipode, S , upgrades the bi-algebra defined by Δ to a Hopf algebra. For any tree $a \in \mathcal{A}$, the antipode, $S(a) \in \mathcal{A}$, is given, again recursively, by [11, 12]

$$S(a) = -a - \sum'_k S(a_k^{(1)}) a_k^{(2)} \quad (6)$$

where \sum'_k omits the terms $a \otimes e$ and $e \otimes a$ of the full Sweedler sum (5). The encoding is

```

procedure S a; sub(A1=S,A2=A1,A1 a-D a);

```

2.3 Counterterm

Renormalization consists in applying an operator R , on the left, at each recursion in the computation of the antipode. In the momentum (MOM) scheme, R_{MOM} is merely the instruction to replace the external momenta by a set of fiducial momenta. In the minimal subtraction (MS) scheme, R_{MS} nullifies external momenta and internal masses and takes only the singular terms of the Laurent expansion in ε . In either case, we have

$$R(R(x)) = R(x) \quad (7)$$

$$R(R(x)R(y)) = R(x)R(y) \quad (8)$$

$$R(x+y) = R(x) + R(y) \quad (9)$$

The counterterm, associated by scheme R to a Feynman diagram with divergence structure given by tree a , is [11, 12]

$$S_R(a) = -R(a) - \sum_k R(S_R(a_k^{(1)})a_k^{(2)}) \quad (10)$$

and is hence encoded by

```
procedure S_R a; R(sub(A1=S_R,A2=A1,A1 a-D a));
```

2.4 Renormalized Green function

The Green-function contribution of a diagram with divergence structure a is

$$\Gamma_R(a) = \lim_{\varepsilon \rightarrow 0} \sum_k S_R(a_k^{(1)})a_k^{(2)} \quad (11)$$

and is hence encoded by

```
procedure G_R a; sub(A1=S_R,A2=A1,D a);
```

which generates 2^n terms in the case of a tree with n vertices, each representing a primitive divergence. The limit $\varepsilon \rightarrow 0$ is not specified in the procedure, but is guaranteed to exist when one provides concrete expressions for the dimensionally regularized bare diagrams, as we shall do in sect. 4.

2.5 Program handsgam.red

The REDUCE program `handsgam.red`, available² via FTP, adds 5 features.

1. A `noncom` instruction prevents reordering of sublists. This is useful in cases where one needs to take account of spin structure.
2. The linearity of R is declared by `let` statements.
3. The loop number of a tree is computed by adding the loop numbers of its primitive decorations. This is included as an argument of R , to facilitate Laurent expansion in the MS scheme.
4. Results for Δ , S_R and Γ_R are stored, to speed up batch processing of diagrams with subdivergences in common, and tests of the operator product expansion.
5. A test is made for the arbitrarily decorated tree $\{1, \{2\}, \{3, \{4\}, \{5\}\}, \{6\}\}$, to ensure that the program correctly generates the 64 terms of the BPHZ formalism.

The reader is invited to generate the 64 BPHZ terms by hand, and then to estimate how long it might take to generate 24,213,878 BPHZ terms for the 7,813 diagrams of sect. 4, without the assistance of Hopf algebra.

²See <ftp://physics.open.ac.uk/physics/dbroadhu/ha/hareadme.txt> for details.

3 Chen's lemma and the OPE

Suppose we renormalize in the MOM scheme at some fiducial momenta labelled generically by p_1 and evaluate Γ_{MOM} at some different external momenta p_2 . Let $\Gamma_{\text{MOM}}^{(1,2)}(a)$ denote the result for a Feynman diagram with divergence structure a . In [14] it is shown that

$$\Gamma_{\text{MOM}}^{(1,2)}(a) = \sum_k \Gamma_{\text{MOM}}^{(1,0)}(a_k^{(1)}) \Gamma_{\text{MOM}}^{(0,2)}(a_k^{(2)}) \quad (12)$$

where the sum is over the Sweedler decomposition of the coproduct of a , the momenta p_0 are arbitrary, and it is understood that

$$\Gamma_R(b) = \prod_j \Gamma_R(b_j) \quad (13)$$

for a product of trees $b = \prod_j b_j$, in any scheme R .

Identity (12) is readily obtained in the toy model of [11], which represents the Hopf algebra of undecorated trees by iterations of products of integrals. In that particular case, it corresponds to an extension of Chen's lemma [16] for iterated integrals. It further extends to arbitrarily decorated trees, in any field theory. In [14] it is construed as a representation of Wilson's operator product expansion [19] (OPE), whose distinctive feature is to allow one to express matrix elements as sums of products with an arbitrary intermediate scale. Here we use (12) as a stringent test of our code: program `hamompe.red` verifies this MOM-scheme OPE.

There is a further result, for the MS scheme. Consider a Feynman diagram, with divergence structure a , contributing to a massless two-point function, with a single external momentum³ p . Then the MS-renormalized result will be a polynomial, $\Gamma_{\text{MS}}(a, L_\mu)$, in $L_\mu := \log(\mu^2/p^2)$, with degree equal to the loop number, where μ is the renormalization scale of the MS scheme. The MOM-renormalized result will be a different polynomial, $\Gamma_{\text{MOM}}(a, L_1)$, in $L_1 := \log(p_1^2/p^2)$, where p_1 is the fiducial momentum. However, there is a strong connection between the sets of MS and MOM polynomials for the terms in the Sweedler decomposition of the coproduct $\Delta(a)$, namely

$$\Gamma_{\text{MS}}(a, L_\mu - L_1) = \sum_k \Gamma_{\text{MS}}(a_k^{(1)}, L_\mu) \Gamma_{\text{MOM}}(a_k^{(2)}, -L_1) \quad (14)$$

with the MOM-scheme results serving to transform MS-scheme results, at momentum p , to a MS-scheme result with momentum p_1 .

We shall apply (14) as a check of our methods in sect. 4. After checking that the calculus passes this test, one may economize by computing the MS results at $p^2 = \mu^2$, since their dependence on external momentum, determined by the renormalization group, is generated by the MOM-scheme results, by setting $L_\mu = 0$ in (14).

4 Hopf algebra of undecorated rooted trees

We now specialize to the Hopf algebra of undecorated rooted trees, generated by a single primitive divergence. From the point of view of pQFT, this is a drastic step: the renor-

³We adopt a metric such that $p^2 > 0$ in the spacelike region.

malized Green functions of the theory, at a given order n , are obtained by computing all decorations with total loop number n and then combining them with the weights given by Wick contractions of the perturbative expansion; little interest might seem to attach to a set of Feynman diagrams with only one-loop primitive propagator subdivergences.

In fact there are (at least) 6 cogent reasons for studying such diagrams.

1. Analytic results for such bare diagrams are immediately available, in terms of highly structured products and quotients of

$$\Gamma(1 - z) = \exp(\gamma z + \sum_{s>1} \zeta(s) z^s / s) \quad (15)$$

where z is an integer multiple of ε , γ is Euler's constant, and $\zeta(s) := \sum_{k>0} 1/k^s$ is the Riemann zeta function. Hence we shall be able to obtain explicit results, of an analytically nontrivial character, for 7,813 diagrams with loop numbers $n \leq 12$, entailing the irreducible zeta values $\{\zeta(3), \zeta(5), \zeta(7), \zeta(9), \zeta(11)\}$ and powers of π^2 from, for example, $\zeta(12) = 691\pi^{12}/638512875$. At the very least, this provides a healthy workout for our Hopf algebra code. More importantly it enables us to look for structure in the counterterms, lacking in the singularities of bare diagrams.

2. The 12 pure rainbow diagrams in our set of 7,813 correspond to trees in which no vertex has fertility greater than unity. They have a remarkable feature, observed in [20] and proved to all orders in [21, 22]: their MS counterterms are rational polynomials in $1/\varepsilon$, bearing no trace of the derivatives of $\log \Gamma(1 - z)$ at $z = 0$, despite the appearance of odd zeta values and powers of π^2 at every step of the BPHZ formalism. This potent example of the simplicity of counterterms was the stimulus for the investigations of [23, 24, 25, 26, 27, 28, 29, 30], where we discovered remarkable features of the nexus of knot/number/field theory [31].
3. Trees in which only the root has fertility greater than zero come from pure chains of one-loop self-energy divergences. In the case of QED these generate the ultra-violet Landau singularity of the photon propagator. In the case of heavy-quark effective theory (HQET) they produce a renormalon structure [32] that frustrates unambiguous Borel resummation of the perturbation series.
4. We may probe even deeper into the number-theory content of the complex of all nestings of rainbows and chains, constituting the full Hopf algebra of undecorated rooted trees, by embedding it inside a two-loop diagram, as was done merely for chains in [33]. Then we will encounter irreducible multiple zeta values [34, 35, 36, 37] of the types $\zeta(5, 3) := \sum_{m>n>0} 1/m^5 n^3$ and $\zeta(3, 5, 3) := \sum_{k>m>n>0} 1/k^3 m^5 n^3$, associated by pQFT to the unique positive 3-braid 8-crossing knot and the unique positive 4-braid 11-crossing knot, in the 7-loop analysis of [23].
5. Next, and most excitingly, this seemingly trivial set of Feynman diagrams was shown in [12] to provide a solution of a universal problem in Hochschild cohomology.
6. Finally, and most intriguingly, there is a unique combination of these diagrams at loop number n which represents a grading of the commutative part of the Hopf

algebra \mathcal{H}_T of the diffeomorphism group [12]. Specifically, if one adds the diagrams with integer weights derivable from work by Connes and Moscovici [17], one expects to see some simpler structure, the details of which neither they nor we anticipated. Thanks to the discovery machine developed in this section, we shall have an interesting result to report in sect. 5, with implications for the relation between noncommutative geometry and quantum field theory.

4.1 Enumeration of rooted trees

The numbers, $N(n)$, of rooted trees with n vertices form a sequence beginning [38]

1, 1, 2, 4, 9, 20, 48, 115, 286, 719, 1842, 4766, 12486, 32973, 87811, 235381, 634847

which grows exponentially, giving

N(250) = 517763755754613310897899496398412372256908589980657316271
041790137801884375338813698141647334732891545098109934676

trees with 250 vertices. Already one sees a nontrivial feature of the iterated structure: tree=root+branches, with every branch being itself a tree. The asymptotic growth

$$N(n) = \frac{b}{n^{3/2}}c^n(1 + O(1/n)) \quad (16)$$

entails constants

b = 0.43992401257102530404090339143454476479808540794011
98576534935450226354004204764605379862197779782334...
c = 2.95576528565199497471481752412319458837549230466359
65953504724789059647331395749510866682836765813525...

that do not appear to be algebraic numbers, since neither the PSLQ [39] nor the LLL [40] algorithm was able to find rational polynomials that fit the first 100 digits and correctly predict the next 10. The origin of their (presumed) transcendentalities resides in the functional equation

$$\log A(x) - A(x) = \log x + \sum_{k>1} \frac{A(x^k)}{k} \quad (17)$$

for the generating function $A(x) := \sum_{n>0} N(n)x^n$, which develops a square-root branch-point at $x = 1/c$, near to which $1 - A(x) \sim \sqrt{1 - cx}$. Setting $x = 1/c$ we obtain

$$\log c = 1 + \sum_{k>1} \frac{A(c^{-k})}{k} \quad (18)$$

which allows one to determine c , by iterative solution, to an accuracy of about $1/N(250) = O(10^{-114})$, after determining $\{N(n) \mid n \leq 250\}$ from (17), at small x . Then Taylor expansion at $x = 1/c$ yields

$$2\pi b^2 = 1 + \sum_{k>1} \frac{A'(c^{-k})}{c^k} \quad (19)$$

with the regularity of the r.h.s. of (17) forcing nonlinear relations between the coefficients, c_k , of $A(x) = 1 - \sum_{k>0} c_k(1 - cx)^{k/2}$.

We hope that these asymptotic results may help colleagues to identify the Lie algebra dual to the Hopf algebra \mathcal{H}_R of rooted trees, which solves a universal problem in Hochschild cohomology [12].

4.2 A variety of models

We shall consider 10 models that generate values for the bare diagrams: 6 of these correspond to well-defined field theories; the remaining 4 are instructive toy models that probe the analytic structure of bare and renormalized diagrams, while ignoring fine details produced by spin and gauge dependence.

4.2.1 BPHZ model

In [11] a BPHZ toy model was developed, by iteration of products of integrals. To each tree, a , it assigns a dimensionally regularized bare value, $B(a)$, obtained by the recursion

$$B(a) = B_n(\varepsilon) \prod_k B(b_k) \quad (20)$$

where n is the number of vertices of a ; b_k are the trees formed from its branches; and

$$B_n(\varepsilon) = \frac{L(\varepsilon, n\varepsilon)}{n\varepsilon} \quad (21)$$

where $L(\varepsilon, \delta)$ is regular at both $\varepsilon = 0$ and $\delta = 0$. This structure is generic; it covers all the field theories that we study. The BPHZ model is a toy only because of the simplicity of its master function, which is

$$L_{\text{BPHZ}}(\varepsilon, \delta) = \frac{\pi\delta}{\sin \pi\delta} \lambda^{-\varepsilon} \quad (22)$$

resulting from nullifying all dimensionful parameters except for an infra-red regulator, λ , in the outermost integration.

4.2.2 Heavy-quark model

More realistically, consider the propagator of a heavy quark in HQET, at virtuality $\omega < 0$. Neglecting a rational function of ε and δ , which we later restore, the master function is

$$L_{\text{HQ}}(\varepsilon, \delta) = \frac{\Gamma(1 - \varepsilon)\Gamma(1 + 2\delta)}{\Gamma(1 - 2\varepsilon + 2\delta)} (-2\omega)^{-2\varepsilon} \quad (23)$$

whose Γ functions are immediately apparent in [41].

4.2.3 Covariant QFT model

For a massless-quark propagator in QCD, with spacelike momentum p , the Γ functions in [6] give

$$L_{\text{QFT}}(\varepsilon, \delta) = \frac{\Gamma(1 - \varepsilon)\Gamma(1 - \delta)\Gamma(1 + \delta)}{\Gamma(1 - \varepsilon - \delta)\Gamma(1 - \varepsilon + \delta)}(p^2)^{-\varepsilon} \quad (24)$$

with a rational factor which will be supplied later.

4.2.4 MZV model

To get multiple zeta values [27] (MZVs) in the bare diagrams, we may embed the full complex of chains and rainbows in a two-loop diagram, as was done for pure QED chains in [33]. Here, we embed it in a finite diagram, so as to remain within the undecorated Hopf algebra. This corresponds to using the recursive process (20,21,24), to compute an n -loop bare value for a covariant propagator diagram, and then multiplying by

$$L_n(\varepsilon) := \frac{2L_{\text{QFT}}(\varepsilon, (n+1)\varepsilon)L_{\text{QFT}}(\varepsilon, (n+2)\varepsilon)}{(n+1)(n+2)\varepsilon^2} S(0, -\varepsilon, (n+1)\varepsilon, -(n+2)\varepsilon) \quad (25)$$

where eq. (17) of our paper with John Gracey [26] gives the general result for the 2-loop 2-point function $S(a, b, c, d)$, which generates MZVs via a ${}_3F_2$ hypergeometric series. With $n_1 + n_2 = n_3 + n_4$, we have $S(n_1\varepsilon, n_2\varepsilon, n_3\varepsilon, n_4\varepsilon) = 3(n_1n_2 - n_3n_4)\varepsilon^2\zeta(3) + O(\varepsilon^3)$, and hence obtain irreducible MZVs at level $n + 2$ in the MS counterterms from undecorated trees with $n \geq 6$ loops. At $n = 9$ we probe as deeply into the relation between knots and numbers as we did in [23]; at $n = 10$, we reach the 12-crossing knots of [26, 27], which revealed an unexpected connection between MZVs and alternating Euler sums [35].

4.2.5 Field theories

As already indicated, we have only to supply a rational function of ε and δ to convert (23) to the realistic case of a heavy-quark propagator in HQET. In an arbitrary covariant gauge, with a gluon propagator $g_{\mu\nu}/q^2 + (\chi - 1)q_\mu q_\nu/q^4$, we obtain

$$L_{\text{HQET}}(\varepsilon, \delta) = \frac{3 - 2\varepsilon - (1 - 2\varepsilon)\chi}{1 - 2\delta} L_{\text{HQ}}(\varepsilon, \delta) \quad (26)$$

which is divergence-free in Yennie gauge, with $\chi = 3$. We may compute in an arbitrary gauge, and also specialize to

$$L_{\text{HQF}}(\varepsilon, \delta) = \frac{2}{1 - 2\delta} L_{\text{HQ}}(\varepsilon, \delta) \quad (27)$$

in Feynman gauge, with $\chi = 1$, and

$$L_{\text{HQL}}(\varepsilon, \delta) = \frac{3 - 2\varepsilon}{1 - 2\delta} L_{\text{HQ}}(\varepsilon, \delta) \quad (28)$$

in Landau gauge, with $\chi = 0$.

Similarly, we can convert (24) to the realistic case of a light-quark propagator in QCD. The master function vanishes, identically, in Landau gauge. Hence we compute in Feynman gauge, with

$$L_{\text{QCD}}(\varepsilon, \delta) = -\frac{2(1-\varepsilon)(1-\delta)}{(1-\varepsilon-\delta)(2-\varepsilon-\delta)}L_{\text{QFT}}(\varepsilon, \delta) \quad (29)$$

For the fermion propagator in Yukawa theory we have

$$L_{\text{Yuk}}(\varepsilon, \delta) = -\frac{2(1-\delta)}{(1-\varepsilon-\delta)(2-\varepsilon-\delta)}L_{\text{QFT}}(\varepsilon, \delta) \quad (30)$$

and for ϕ^3 theory, in $6 - 2\varepsilon$ dimensions, we obtain

$$L_{\text{phi}}(\varepsilon, \delta) = -\frac{6(1-\varepsilon)}{(1-\varepsilon-\delta)(2-\varepsilon-\delta)(3-\varepsilon-\delta)}L_{\text{QFT}}(\varepsilon, \delta) \quad (31)$$

after removing irrelevant multiples of the couplings.

Thus one chooses a theory, or toy, by setting the `model` switch to one of the 10 values `{bphz, hq, qft, mzv, hqet, hqf, hql, qcd, yuk, phi}`, corresponding to the processes (22–31).

4.3 A variety of schemes

We shall investigate the 10 models in 9 renormalization schemes. This multiplicity of schemes results from a pair of ternary switches, `mscheme` and `gscheme`, each of which may take the values 0, 1, or 2.

4.3.1 Momentum, minimal and nonminimal schemes

Our first ternary switch, `mscheme`, chooses between the MOM scheme, the MS scheme, and a nonminimal scheme (NMS).

With `mscheme:=0`, we retain the full ε dependence of the bare diagrams and generate counterterms by replacing the external momentum by a fiducial momentum.

With `mscheme:=1`, we retain in the counterterms only the singular terms of the Laurent expansion, after nullifying dimensionful parameters.

With `mscheme:=2`, we retain the finite term as $\varepsilon \rightarrow 0$, in addition to the singular MS terms. Such finite counterterms occur in the delicate handling of γ_5 in dimensional regularization [32, 42]. Like the MOM and MS schemes, this NMS scheme satisfies (8).

4.3.2 G schemes

In [43] it was observed that the appearance of π^2 (but not of π^4) may be suppressed, in covariant field theory, by absorbing suitable Γ functions into the D -dimensional coupling, which already absorbs the universal factor $1/(4\pi)^{D/2}$. Our second ternary switch, `gscheme`, reflects this freedom.

With `gscheme:=0`, we leave the master function (22) as it stands and modify (23,24) only by including the canonical $\overline{\text{MS}}$ factor $\exp(\gamma\varepsilon)$, which suppresses Euler’s constant, γ .

With `gscheme:=1`, we divide the master functions (22–24) by their values at $\delta = \varepsilon$ and unit scale, thus obtaining $B_1(\varepsilon) = 1$ for the one-loop diagram, when the scale — i.e. λ in (22); -2ω in (23); or p^2 in (24) — is set to unity. This suppresses γ in the HQ and QFT cases, and also $\zeta(2) = \pi^2/6$ in the QFT case. We know from [41] that π^2 is intrinsic to HQET counterterms.

With `gscheme:=2`, we leave the master function (22) as it stands and multiply (23,24) by $\Gamma(1 - \varepsilon)$. This likewise suppresses γ in the HQ and QFT cases, and also $\zeta(2) = \pi^2/6$ in the QFT case, yet it leaves a nontrivial value for the one-loop term $B_1(\varepsilon)$ and hence seems less contrived than the G scheme in [43].

We believe that the 9 schemes entailed by our pair of ternary switches subsume much of current practice in pQFT. We make no attempt to implement dimensional reduction, analytic regularization, or differential renormalization, though these appear to present no problem of principle to the global description of [11, 12].

4.4 Computational strategy

There are $\sum_{n=1}^{12} N(n) = 7,813$ undecorated diagrams with $n \leq 12$ loops. To obtain their renormalized values we must compute $\sum_{n=1}^{12} 2^n N(n) = 24,213,878$ BPHZ terms. To do this in 10 models and 9 renormalization schemes would require us to process more than 2×10^9 BPHZ terms, with n th order polynomials of a logarithm appearing at n loops. These polynomials entail $90 \sum_{n=1}^{12} 2^n (n+1) N(n) = 27,804,356,640$ coefficients. These coefficients contain, in general, products of odd zeta values and powers of π^2 . The number of rational coefficients of such products is $90 \sum_{n=1}^{12} 2^n N(n) \sum_{k=0}^n C(k) = 335,708,683,560$, where the multiplicity, $C(k)$, of zeta products with levels up to k forms the sequence

$$1, 1, 2, 3, 4, 6, 8, 11, 14, 19, 24, 31, 39, 49, 61, 76$$

for $0 \leq k \leq 15$, neglecting the proliferation of the irreducible MZVs of model (25), which increases these integers to give partial sums of the Padovan sequence [27]. Many of these 3.3×10^{11} rationals will be ratios of integers with $O(10)$ decimal digits. From this, it is apparent that a complete analysis, up to 12 loops, might entail processing several terabytes⁴ of exact integer data. Thus computational efficiency is at a premium.

Clearly, the best strategy for any computation that involves all 7,813 diagrams is an Aufbau, in which results at n loops are held in core memory, and then used at $n+1$ loops, with only a single new recursion of the algorithms (2,6,20) for the coproduct, antipode and bare diagrams. To achieve a 12-loop renormalized result, one needs to hold 13 terms from each Laurent expansion, at every loop number $n < 12$, but need not hold the results for the majority of diagrams, namely those 4,766 with $n = 12$, if only weighted totals, such as those presented in sect. 5, are required as output.

⁴For loop numbers $n \leq 15$, we would be talking of petabytes.

4.5 Results and timings

As benchmarks, we present timings for obtaining the renormalized values for all diagrams up to a given loop number. As interesting weights, for the output of results, we choose those suggested by the work of Connes and Moscovici [17] (CM) and derived in sect. 5. We emphasize that these weighted results were obtained by summing over the results in the full Hopf algebra of undecorated trees, not by specializing to the CM case *ab initio*.

Allocating 128MB of core memory to REDUCE on a 533MHz DecAlpha machine we computed the case `model:=bphz; mscheme:=0; gscheme:=0`. The 10-loop CM-weighted counterterm, at scale $\lambda = 1$, has finite part

$$S_{10}^{\text{CM,finite}} = -\frac{214046911\pi^{10}}{2112} \quad (32)$$

obtained in less than 2 minutes. The 12-loop result

$$S_{12}^{\text{CM,finite}} = -\frac{43556707893701\pi^{12}}{1048320} \quad (33)$$

took less than 2 hours. We would be interested to learn of any method that can obtain this result, from explicit computation of all 7,813 counterterms at loop numbers $n \leq 12$, in a significantly shorter time.

The next step was to test the code against the MOM-scheme OPE (12), which was verified, as were the MS-scheme OPE (14) and its NMS-scheme version

$$\Gamma_{\text{NMS}}(a, L_\mu - L_1) = \sum_k \Gamma_{\text{NMS}}(a_k^{(1)}, L_\mu) \Gamma_{\text{MOM}}(a_k^{(2)}, -L_1) \quad (34)$$

Thus we may economize, by computing only MOM-scheme results at arbitrary momentum, while $p^2 = \mu^2$ suffices in the MS and NMS cases, thanks to the renormalization group. This helps to keep the memory requirements within practical bounds, since the MOM-scheme renormalized Green-function contributions are clearly rational polynomials of a log, and are independent of the `gscheme` switch.

The modifications of spin and gauge-dependence, in (26–31), introduce no new analytic feature; they merely proliferate terms by mixing products of zeta values with different levels. Hence we were content to compute theories (27–31) to 10 loops. We omitted the arbitrary-gauge case (26), which generates polynomials of degree n in χ at n loops. We postpone presentation of results for the MZV model (25) to a later publication, which will address the associated knot theory [23, 24, 26, 27].

At 11 loops, we encountered no difficulty in processing models (22–24); at 12 loops, 128MB of core memory was sufficient only to process model (22). In Table 1 we present the times (to the nearest minute) taken to compute all the counterterms and renormalized values up to the specified loop number, at $p^2 = \mu^2$ in the MS scheme, with `gscheme=1`, in 8 models. All timings refer to REDUCE3.5, which was allocated 128MB of core memory on a 533MHz DecAlpha; changes of scheme have little effect on them. Results for the CM-weighted counterterms and renormalized Green functions are in the

12 files `ha<model><loops>.out`. In `haphi10.out` one encounters, *inter alia*, a 25-digit integer with a 22-digit prime factor.

Table 1: Time taken to compute all MS counterterms and renormalized values.

model	bphz	hq	qft	hqf	hql	qcd	yuk	phi	bphz	hq	qft	bphz
loops	10	10	10	10	10	10	10	10	11	11	11	12
minutes	3	7	5	15	15	11	10	14	17	39	31	124

5 Connes-Moscovici weights

In [12] an important connection was found between the Hopf algebra \mathcal{H}_T of the diffeomorphism group, studied by Connes and Moscovici [17], and the Hopf algebra \mathcal{H}_R of undecorated rooted trees [11], for which we now have 10 representations, generated by (22–31). The commutative part of \mathcal{H}_T is a subalgebra of \mathcal{H}_R . Along with the obvious rainbow subalgebra of [20], it exhausts [12] the proper Hopf subalgebras of \mathcal{H}_R . In consequence, there exist nonzero CM weights for our 7,813 diagrams, such that summing n -loop diagrams with these weights, we arrive at representations of the grading of the CM subalgebra, with results for the counterterms that we expect to be as distinctive as for the rainbow diagrams in [20].

5.1 Computation of CM weights

The CM weights are defined as follows. Suppose that one has the CM combination at loop number n . To generate the CM combination at loop number $n + 1$, one grows each previous tree to form n new trees, by attaching a new vertex to each of the original vertices, in turn. The starting point, at $n = 1$, is the unique branchless rooted tree, with CM weight $W(\{1\}) = 1$. It is not difficult to encode this algorithm, to obtain the CM weights for the 7,813 trees with $n \leq 12$, though our first encoding ran for more than an hour, until it had finally distributed $11! = 39,916,800$ terms between the 4,766 CM weights of 12-loop diagrams. The results are in the file `hagenhaw.out`, with a coding of diagrams given in `hagendum.out`.

The defining algorithm for these CM weights appears to be very different from those for the coproduct and antipode of \mathcal{H}_R . For the latter, we could write simple algorithms that were blind, at any given recursion, to all structure save that immediately below the root (or head) of the tree. By contrast, CM weights appear to feel all the way down to the last vertices of the trees, which we refer to as feet⁵. An efficient head-first algorithm for the CM weight, $W(t)$, was not easy to find. We finally achieved it, as follows.

The CM definition translates to the feet-first recursion

$$W(t)\Pi(t) = \sum_j W(f_j)\Pi(f_j) \tag{35}$$

⁵Recall that a mathematical tree has, like a family tree, its root at the top.

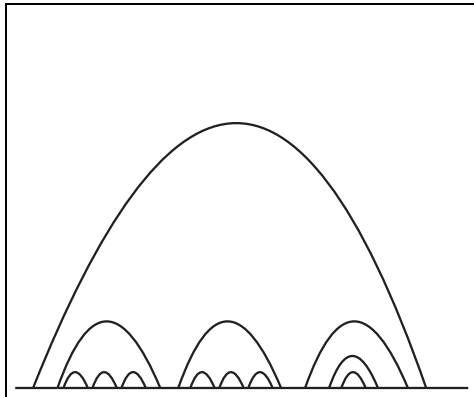


Figure 3: A 12-loop diagram based on a one-loop skeleton.

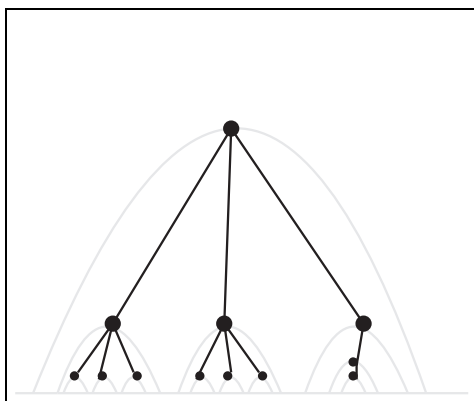


Figure 4: The divergence structure of Fig. 3, exhibiting permutation symmetry.

where the f_j are all the trees obtained by removing a single foot from t , and $\Pi(t)$ is a permutation factor, equal to the number of trees that are indistinguishable from t by permutations of branches originating from any vertex. For example, the 12-loop Feynman diagram of Fig. 3 has a permutation⁶ factor $\Pi(t_{12}) = 2! \times 3! \times 3! = 72$, as is apparent from its divergence structure

$$t_{12} := \{1, \{1, \{1\}, \{1\}, \{1\}\}, \{1, \{1\}, \{1\}, \{1\}\}, \{1, \{1, \{1\}\}\}\} \quad (36)$$

illustrated in Fig. 4.

Now the remarkable thing about the defining formula (35) is that it produces no prime factor greater than $n - 1$, for a tree with n vertices. This is not at all clear from the formula, since the sum seems to allow the possibility of adding, let us say, the integers 9 and 4, to obtain the forbidden prime 13. To show that this cannot happen, we define another construct: the tree factorial, $t^!$. Its recursive definition is

$$t^! = n \prod_k b_k^! \quad (37)$$

where n is the number of vertices of t and b_k are its branches. In the pure rainbow case, where no vertex has fertility greater than unity, $t^!$ is the ordinary factorial of the number of vertices, n . In the case of Fig. 4, we have $t_{12}^! = 12 \times 4 \times 4 \times 3! = 1152$.

⁶This permutation factor is quite distinct from any field theoretic symmetry factor.

So now we have a feet-first sum for the CM weights (35), and a head-first product for the tree factorial (37). The trick is to convert the latter to a feet-first sum, and then express the former as a simple head-first product. In [14] it is proven, by induction, that the tree factorials $b_k^!$ of the beheadings of any tree are related to the tree factorials $f_j^!$ of its befootings by a wonderfully simple formula:

$$\prod_k \frac{1}{b_k^!} = \sum_j \frac{1}{f_j^!} \quad (38)$$

which produces, for example, the equality

$$\frac{1}{4} \times \frac{1}{4} \times \frac{1}{3!} = \frac{6}{11 \times 4 \times 3 \times 3!} + \frac{1}{11 \times 4 \times 4 \times 2} \quad (39)$$

in the case of Fig. 4. Then a second induction gives

$$W(t) = \frac{n!}{t^! \Pi(t)} \quad (40)$$

with $t^!$ given by (37), and $\Pi(t)$ likewise given by a head-first recursion, namely

$$\Pi(t) = \pi(t) \prod_k \Pi(b_k) \quad (41)$$

where $\pi(t)$ is the number of indistinguishable permutations of the branches b_k of t .

This reduces the computation of the CM weight $W(t)$ to a rather simple procedure. One associates a pair of integers to each vertex of a tree: the first is the number of vertices of the subtree with this root; the second is the number of indistinguishable permutations of its branches. For a tree with n vertices, one obtains $W(t)$ from (40) by dividing $n!$ by all these integers. In the case of Fig. 4,

$$W(t_{12}) = \frac{12!}{(12 \times 4 \times 4 \times 3!) \times (2! \times 3! \times 3!)} = 3 \times 5^2 \times 7 \times 11 = 5775 \quad (42)$$

gives the rather nontrivial Connes-Moscovici weight of the Feynman diagram of Fig. 3. Computing the CM weights of all 4,766 12-loop diagrams, and combining results from sect. 4 with these weights, we expect to find something as interesting as the rational rainbow results of [20].

5.2 Results with CM weights

We do indeed find rationality. The Laurent expansion of the 12-loop CM antipode of the BPHZ model (22), at $\lambda = 1$, is

$$S_{12}^{\text{CM}} = \frac{155925}{8\varepsilon^{12}} - \frac{43556707893701\pi^{12}}{1048320} + O(\varepsilon^2) \quad (43)$$

with *no* singular term that entails π . As far as Connes and Moscovici are concerned, the Bernoulli numbers generate no subleading Laurent residues! Moreover this depends upon no property of the Bernoulli numbers. With arbitrary coefficients, C_k , in the expansion

$$B_n(\varepsilon) = \frac{1}{n\varepsilon} \left(1 + \sum_{k>0} C_k (n\pi\varepsilon)^{2k} \right) \quad (44)$$

the 12-loop CM antipode would have the same π -free singularity. Yet the *finite* part of

$$\begin{aligned} S_{12}^{\text{CM}} = & 155925 \left(\frac{1}{8\varepsilon^{12}} - \left\{ 51321600C_6 + 21837600C_5C_1 + 7001856C_4C_2 + 3232224C_4C_1^2 \right. \right. \\ & + 2534490C_3^2 + 2208576C_3C_2C_1 + 229020C_3C_1^3 + 158336C_2^3 \\ & \left. \left. + 146550C_2^2C_1^2 + 9180C_2C_1^4 + \frac{231}{4}C_1^6 \right\} \pi^{12} \right) + O(\varepsilon^2) \end{aligned} \quad (45)$$

shows the nontrivial processing of coefficients that results from the recursions for the coproduct (2), the antipode (6), and the bare diagrams (20), in the presence of the CM weights (40).

With CM weights, the sole singular n -loop counterterm of the BPHZ model (22) is of a rational, diagonal, quadratic form, $W_2(n)/(-\varepsilon)^n$, where

$$W_2(n) := \sum_{k=1}^{N(n)} \frac{W(t_k)}{t_k!} = \frac{1}{n!} \sum_{k=1}^{N(n)} W(t_k) \Pi(t_k) W(t_k) \stackrel{?}{=} \frac{(n-1)!}{2^{n-1}} \quad (46)$$

posits a closed form, for the sum over all trees t_k with n vertices, which we have verified for $n \leq 12$, yet have not proved in general. Moreover, we found that $W_2(n)/(-\varepsilon)^n$ is also the sole n -loop MS counterterm in the CM-weighted QFT model of (24) at $n \leq 11$ loops. The minimal subtraction scheme is such common practice in pQFT because it retains in counterterms only those (products of) zeta values that are strictly necessary to render the renormalized Green functions finite. CM weights combine Feynman diagrams so as to annihilate all zeta values in model (24), just as they annihilate powers of π^2 in model (22).

Inspection of (22) and (24) shows that each is an even function of δ . Thus we investigated the most general Ansatz with this property, namely

$$B_n(\varepsilon) = \frac{1}{n\varepsilon} \sum_{j,k \geq 0} C_{j,k} (n\varepsilon)^{2j} \varepsilon^k \quad (47)$$

The MS counterterm from an individual 10-loop diagram involves up to 302 terms, formed from products of $\{C_{j,k} \mid 0 \leq 2j + k < 10\}$. It took an hour to compute all 719 10-loop counterterms, with symbolic values for the coefficients in (47). Combining them with CM weights, we annihilated 301 products of the arbitrary coefficients, and were left with only the expected multiple, $W_2(10) = 9!/2^9 = 2835/4$, of $(-C_{0,0}/\varepsilon)^{10}$.

We find it significant that the ineluctable divergences of renormalization are so responsive to ideas from noncommutative geometry. This strengthens our opinion that renormalization is of real interest, in its own right, and far from being a cause for regret.

6 Conclusions and prospects

In this paper, we automated the process of renormalization. Its Hopf algebra structure, imposed by the necessity to generate local counterterms, was summarized in a few lines of code. The generality of this algebraic structure extends to the renormalization of realistic particle physics problems, as in the Standard Model. Here, we computed deep into the perturbation expansion in cases where the remaining analysis was straightforward.

Different renormalization schemes and changes of scale were implemented with ease, thanks to the convolutions (12,14). We regard no renormalization scheme as better defined than others; all can be treated on the same algebraic footing. Indeed, it will be shown elsewhere [14, 44] that a minimal subtraction scheme can, for example, be obtained as a BPHZ scheme, whose renormalization scales are indexed by rooted trees.

The results in sect. 5 indicate a deep connection between QFT and noncommutative geometry. There is an index-theoretic flavour, in the annihilation of zeta values by Connes-Moscovici weights, which deserves further study. In particular, the new relation (40), between tree factorials and CM weights, will be of great help in making the connection between counterterms and diffeomorphisms, as was envisaged in [12] and will be made more precise in [45]. We also hope that the asymptotic enumeration of sect. 4.1 will help Lie-algebra specialists to solve the outstanding problem of identifying the dual of \mathcal{H}_R .

Our construction of a renormalization engine demonstrates that the remaining challenges in computational pQFT lie in two related areas: elucidation of algebraic relations [46, 47] between decorations; analysis of those iterated integrals [14], or multiple sums [9], that are the concrete representations of the truly primitive elements which survive this filtration.

We envisage that both endeavours will be illuminated by an interplay [12] with non-commutative geometry [17].

Acknowledgments: We thank the ESI for generous hospitality in Vienna; Alain Connes, Victor Kac and Ivan Todorov for discussions there; Bob Delbourgo and John Gracey for collaborations that contributed to this work; and HUCAM for grant CHRX-CT94-0579, which contributed materially to our meeting over the last 4 years.

References

- [1] N.N. Bogoliubov, O. Parasiuk, *Acta Math.* **97** (1957) 227.
- [2] K. Hepp, *Comm.Math.Phys.* **2** (1966) 301.
- [3] W. Zimmermann, *Comm.Math.Phys.* **15** (1969) 208.
- [4] J. Collins, *Renormalization* (Cambridge Univ. Press, 1986).
- [5] G. 't Hooft, M. Veltman, *Nucl.Phys.* **B44** (1972) 189.
- [6] K.G. Chetyrkin, F.V. Tkachov, *Nucl.Phys.* **B192** (1981) 159;
F.V. Tkachov, *Phys.Lett.* **B100** (1981) 65.
- [7] D.J. Broadhurst, *Z.Phys.* **C54** (1992) 599.
- [8] L.V. Avdeev, *Comput.Phys.Commun.* **98** (1996) 15.
- [9] D.J. Broadhurst, hep-th/9803091, to appear in *Eur.Phys.J. C*;
hep-th/9805025, to appear in *Eur.Phys.J. C*;
hep-th/9806174, submitted to *Eur.Phys.J. C*.
- [10] T. van Ritbergen, J.A.M. Vermaseren, S.A. Larin, *Phys.Lett.* **B400** (1997) 379,
hep-ph/9701390.
- [11] D. Kreimer, *Adv.Theor.Math.Phys.* **2** (1998) 303, q-alg/9707029.
- [12] A. Connes, D. Kreimer, *Hopf Algebras, Renormalization and Noncommutative Geometry*, hep-th/9808042, to appear in *Comm.Math.Phys.*
- [13] D. Kreimer, *On overlapping Divergences*, hep-th/9810022.
- [14] D. Kreimer *Chen's iterated Integral represents the Operator Product Expansion*, in preparation.
- [15] A.C. Hearn, *REDUCE User's Manual*, Version 3.6, RAND publication CP78, July 1995.
- [16] T.K. Chen, *Bull.Amer.Math.Soc.* **83** (1977) 831.
- [17] A. Connes, H. Moscovici, *Hopf Algebras, cyclic Cohomology and the transverse Index Theorem*, IHES/M/98/37, math.DG/9806109.
- [18] J.D. Bjorken, S.D. Drell, *Relativistic Quantum Fields* (McGraw-Hill, New York, 1965).
- [19] K.G. Wilson, *Phys.Rev.* **179** (1969) 1699.
- [20] D. Kreimer, *Phys.Lett.* **B354** (1995) 117, hep-th/9503059.

- [21] R. Delbourgo, A. Kalloniatis, G. Thompson, Phys.Rev. **D54** (1996) 5373, hep-th/9605107.
- [22] R. Delbourgo, D. Elliott, D.S. McAnally, Phys.Rev. **D55** (1997) 5230, hep-th/9611150.
- [23] D.J. Broadhurst, D. Kreimer, Int.J.Mod.Phys. **C6** (1995) 519, hep-ph/9504352.
- [24] D.J. Broadhurst, R. Delbourgo, D. Kreimer, Phys.Lett. **B366** (1996) 421, hep-ph/9509296.
- [25] D. Kreimer, J.Knot Th.Ram. **6** (1997) 479, q-alg/9607022.
- [26] D.J. Broadhurst, J.A. Gracey, D. Kreimer, Z.Phys. **C75** (1997) 559, hep-th/9607174.
- [27] D.J. Broadhurst, D. Kreimer, Phys.Lett. **B393** (1997) 403, hep-th/9609128.
- [28] D. Kreimer, Eur.Phys.J. **C2** (1998) 757, hep-th/9610128.
- [29] D.J. Broadhurst, A.V. Kotikov, hep-th/9612013, to appear in Phys.Lett. **B**.
- [30] D. Kreimer. Acta Phys.Polon. **B29** (1998) 2865, hep-th/9807125.
- [31] D. Kreimer, *Knots and Feynman Diagrams* (Cambridge Univ. Press, in press).
- [32] D.J. Broadhurst, A.G. Grozin, Phys.Rev. **D52** (1995) 4082, hep-ph/9410240.
- [33] D.J. Broadhurst, Z.Phys. **C58** (1993) 339.
- [34] J.M. Borwein, D.M. Bradley, D.J. Broadhurst, Elec.J.Combinatorics. **4** (1997) R5, hep-th/9611004.
- [35] D.J. Broadhurst, hep-th/9604128, to appear in J.Math.Phys.
- [36] J.M. Borwein, D.M. Bradley, D.J. Broadhurst, P. Lisonek, *Special Values of Multidimensional Polylogarithms*, CECM report 98-106, May 1998, submitted to Trans.A.M.S.
- [37] J.M. Borwein, D.M. Bradley, D.J. Broadhurst, P. Lisonek, *Combinatorial Aspects of Euler Sums*, CECM report 98-107, June 1998, to appear in Elec.J.Combinatorics.
- [38] N.J.A. Sloane, *On-line Encyclopedia of Integer Sequences*, sequence A000081, <http://www.research.att.com/~njas/sequences>;
F. Bergeron, G. Labelle, P. Leroux, *Combinatorial Species and Tree-like Structures* (Cambridge Univ. Press, 1998) p. 279.
- [39] H.R.P. Ferguson, D.H. Bailey, S. Arno, *Analysis of PSLQ, an integer relation finding algorithm*, NASA-Ames Technical Report, NAS-96-005, to appear in Math.Comp.

- [40] A.K. Lenstra, H.W. Lenstra, L. Lovász Math. Ann. **261** (1982) 515;
R. Kannan, A.K. Lenstra, L. Lovász, Math. Comp. **50** (1988) 235.
- [41] D.J. Broadhurst, A.G. Grozin, Phys.Lett. **B267** (1991) 105;
Phys.Lett. **B274** (1992) 421.
- [42] D.J. Broadhurst, A.L. Kataev, Phys.Lett. **B315** (1993) 179, hep-ph/9308274
- [43] K.G. Chetyrkin, A.L. Kataev, F.V. Tkachov, Nucl.Phys. **B174** (1980) 345.
- [44] R. Delbourgo, D. Kreimer, in preparation.
- [45] A. Connes, D. Kreimer, in preparation.
- [46] D. Kreimer, J.Knot Th.Ram. **7** (1998) 61, hep-th/9612010.
- [47] D.J. Broadhurst, D. Kreimer, Phys.Lett. **B426** (1998) 339, hep-th/9612011.